An electrochemically switchable triiodide-ion-imprinted PPy membrane for highly selective recognition and continuous extraction of iodide

Jinhua Luo[a], Xiao Du[a], Fengfeng Gao[a], Haixia Kong[b], Xiaogang Hao[a,*], Abuliti Abudula[c], Guoqing Guan[c, d,], Xuli Ma[e], Bing Tang[f]**

[a] *Department of Chemical Engineering, Taiyuan University of Technology, Taiyuan, 030024, P. R. China*

[b] *China Institute of Radiation Protection, Taiyuan, 030006, P. R. China*

[c] *Graduate School of Science and Technology, Hirosaki University, Hirosaki 036-8560, Japan.*

[d] *Energy Conversion Engineering Group, Institute of Regional Innovation (IRI), Hirosaki University, 2-1-3 Matsubara, Aomori 030-0813, Japan*

[e] *College of Environmental Science and Engineering, Taiyuan University of Technology, Jinzhong, 030600, China*

[f] *School of Environmental Science and Technology, Guangdong University of Technology, Guangzhou,510006, P. R. China*

([*]xghao@tyut.edu.cn; [**]guan@hirosaki-u.ac.jp)

Abstract

An electrochemically switchable triiodide-ion-imprinted polypyrrole (PPy/I_3^-) membrane composed of uniform bowl-shape particles with an interconnected ant-nest-like structure was successfully developed for the highly selective recognition and continuous extraction of iodide from the aqueous solutions in a novel electrochemically switched ion membrane extraction (ESIME) process. As a result, the PPy/I_3^- membrane

with the ESIME process displayed a high I^- ion flux of 2.87×10^{-4} $g\cdot cm^{-2}\cdot h^{-1}$, high separation factors of 3.44, 3.98, 5.02 and 5.27 for I^- over Br^-, Cl^-, SO_4^{2-} and PO_4^{3-} anions, respectively, and excellent cycling stability with an extraction efficiency of 94.8% even after 10-cycle reuse at the optimized conditions with a cell voltage of 1.8 V, a pulse potential of -0.8 V/+0.95 V, a pulse width of 20 s. It is expected that the PPy/I_3^- membrane with ESIME process could be a promising candidate for the continuous, efficient and eco-friendly extraction of target I^- from industrial water system.

Keywords: triiodide ion imprinted; polypyrrole membrane; electrochemically switched ion membrane extraction; continuous extraction; radioactive iodine

1. Introduction

I^{131} is an important radioisotope of iodine, which is used extensively in the nuclear power industry, medical research and other fields [1-3]. However, once ingested, it can accumulate in the body, particularly the thyroid gland, increasing the risk of thyroid cancer. Thus, how to securely handle them becomes an important issue [4-10]. Meanwhile, radioactive iodine is used in the treatment of hyperthyroidism and some cutting-edge medicine fields [11, 12]. Hence, the effective extraction and the use of radioactive iodide play an irreplaceable important role in the rapid and healthy development of nuclear power. To date, various methods such as adsorption [13-15], precipitation [16-20], membrane processes [3, 21] and ion exchange [22-24] have been developed to capture the I^-. Among them, ion exchange way should be a relatively simple, safe and low-cost process [2, 25, 26]. In contrast, other ones always have high-cost and secondary pollution, limiting the large-scale and environmental-friendly applications.

In recent years, as an eco-friendly ion extraction technique, electrochemically switched ion exchange (ESIX) technique [22, 27-31] has gained great attention. Especially, the reversible adsorption and desorption of the target ions can be controlled by changing the redox state of ESIX film, so that the used film will be easily regenerated and without any secondary wastes in the process. various kinds of ESIX films have been developed in our previous work, and used for the extraction of different target anions [32-34] and cations [30, 31, 35] in aqueous solutions with low concentrations. Nevertheless, the traditional ESIX technique is a non-continuous operation process, in which the recovery process of ESIX film need to be operated intermittently in each ion uptake/release cycle. To realize a continuous operation process, we have also developed an electrochemically switched ion permselective (ESIP) technique to continuously recover the target metal ions [36-40].

In this study, I^- ions can be easily oxidized into I_2 molecules at an oxidation potential, and then rapidly combined with I^- ions to form I_3^- ions. Combined ESIP technology with a special redox reaction between I^- and I_3^- ions, we designed a novel electrochemically switched ion membrane extraction (ESIME) process used for continuous extraction of target I^- ions. Herein, an ESIME membrane with higher selectivity and excellent extraction capacity for I^- ions is the crucial task for the practical application was designed. In our previous study, to capture of the I^- ions effectively, an iodide ion trapping polypyrrole (PPy) film with the electrochemically switched ion extraction (ESIE) ability was synthesized based on the special PPy properties [23, 28, 41-43], which demonstrated a high extraction capacity and remarkable selectivity toward the I^- ions. Thus, in this study, in order to improve the extraction capacity and reinforce I^- ion trapping effect , a triiodide ion imprinted PPy membrane (PPy/I_3^-) was designed.

As shown in Fig. 1, in the present designed ESIME process, when the oxidation potential is performed on the membrane, the oxidation/protonation of nitrogen atoms will be generated in PPy. Meanwhile, a positively charged appeared on the PPy membrane, which elicited oriented locomotion of target I^- ions from the source cell chamber to the membrane, and then the I^- will be absorbed on the PPy membrane. Conversely, when a reduction potential is applied on the PPy membrane, the positive charge of PPy disappears, moreover, coupled with a cell voltage, I^- ions will be rapidly released into the receiver cell chamber from the membrane. Herein, in the I^- ion adsorption process, I^- ions will be firstly oxidized into I_2 molecules, and then combined with I^- ions to form I_3^- ions, which will be subsequently trapped into the membrane rapidly. Conversely, when a reduction potential is performed on the PPy membrane, the I_3^- ions will be reduced to I^- ions before desorbed into the receiving cell chamber, which is beneficial for the rapid desorption of I^- ions. As such, by repeatedly operation of the above process, I^- ions can be continuously extracted from the source cell chamber to the receiver cell chamber via the electroactive PPy/I_3^- membrane.

In this work, the electroactive PPy/I_3^- membrane composed of uniform bowl-shape particles with an interconnected ant-nest-like structure was synthesized and used in the ESIME technique for selective recognition and continuous extraction and recovery of I^- ions. The influence factors (such as cell voltage and pulse width) on the extraction properties were investigated. Furthermore, the performances for extraction of I^- ions from the aqueous solutions in the presence of other anions including Cl^-, Br^-, SO_4^{2-} and PO_4^{3-} were studied. Meanwhile, the ESIME mechanism related to the coupling of electrochemical redox reaction with the ion exchange process was proposed to explain the enhanced I^- ion extraction efficiency. It is expected to build an extraction- reaction -desorption mechanism model of such an electroactive membrane and provide a

guidance to address a practical ion extraction system.

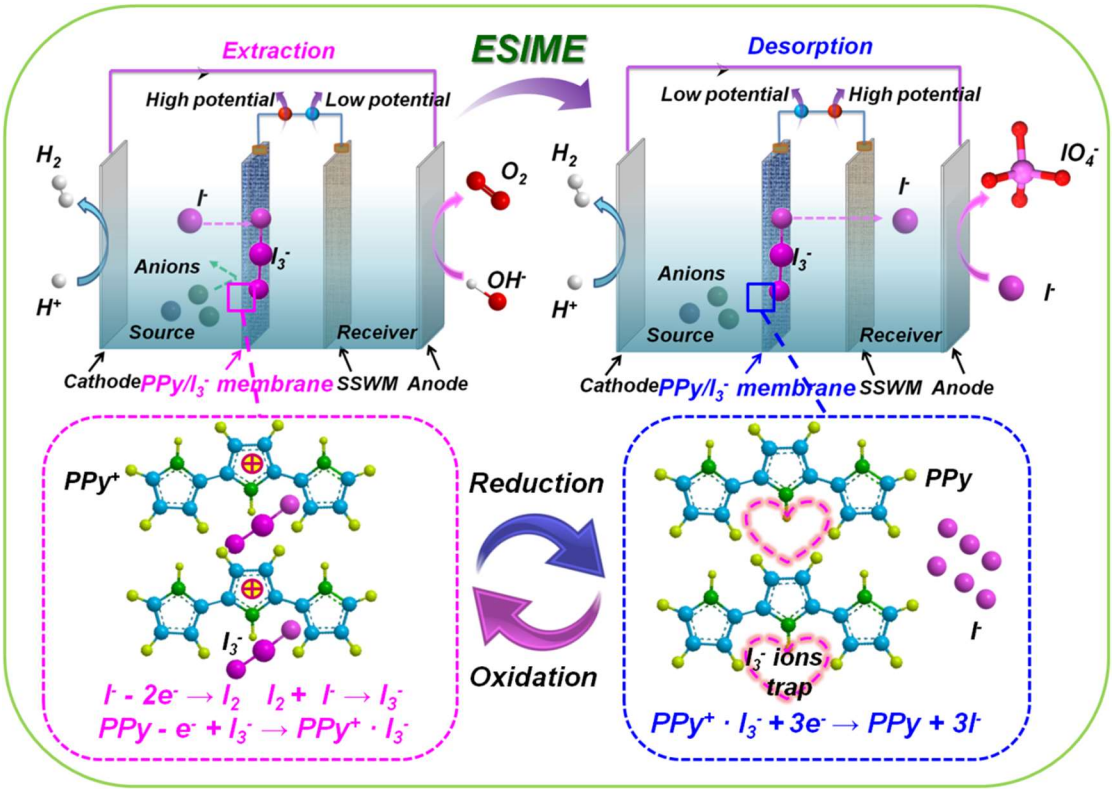

Fig. 1. Schematic illustration of the electrochemically switched ion membrane extraction (ESIME) system, taking the extraction of I^- ions using electroactive PPy/I_3^- membrane.

2. Experimental section

2.1 Synthesis of PPy/I_3^- membrane

The PPy/I_3^- membrane was prepared by a one-step electrodeposition way based on a three-electrode structure which comprised a 3 cm × 3 cm stainless steel wire mesh (SSWM) working electrode, a Pt auxiliary electrode and a Ag/AgCl reference electrode. In the PPy/I_3^- membrane preparation process, 30 mL of 0.1 M pyrrole aqueous solution containing 0.4 M KI_3 was used as the electrolyte, in which the I_3^- solution was prepared by dissolving proportional I_2 in KI solution at first. The operation potential for the membrane preparation was applied at +0.9 V. The obtained PPy/I_3^- coated SSWM

electrode was rinsed with distilled water to eliminate the rest of the pyrrole monomer and electrolyte. Fig. 2 illustrates the imprinting of I_3^- ions in the PPy during the electrochemical oxidation polymerization process.

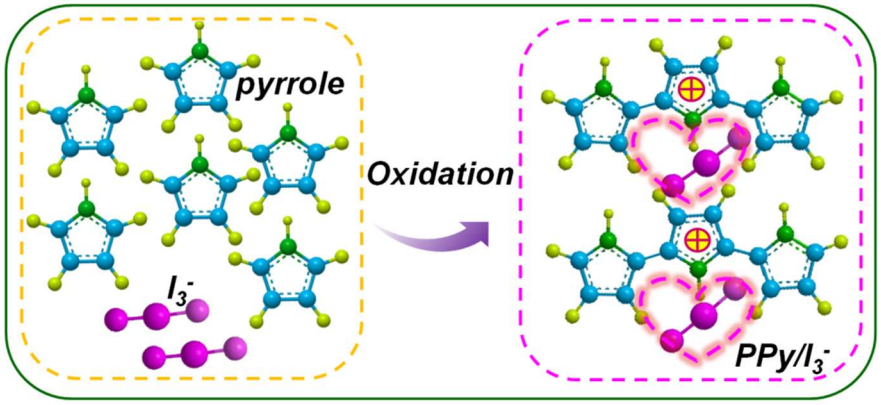

Fig. 2. Schematic diagram of electrochemical oxidation polymerization process during PPy/I_3^- membrane preparation.

2.2 ESIME module

The ESIME module was composed of two cell chamber as shown in Fig. 1. In the middle of the cell chamber to install a PPy/I_3^- coated SSWM which can be as powerful curtain between source and receiver cell, as well as served as the working electroactive membrane for the efficient extraction of target I^- ions. Herein, the actual membrane area was about 0.75 × 0.75 × π cm^2, and the volume of each cell chamber was 30 mL. Moreover, the ESIME system includes two subsystems as follows: cell voltage system and pulse potential system, in which the cell voltage was performed at a couple of 2 ×10 cm^2 stainless steel plates electrode to enhance the directional ion migration rate, while the pulse potential was performed at the PPy/I_3^- membrane electrode and the blank SSWM auxiliary electrode.

2.3 Continuous extraction test

Before the continuous extraction test, the imprinted I_3^- need to be removed at a

constant voltage of -0.8 V to form a new I_3^- ion trapping PPy membrane. Subsequently, mounting the I_3^- ion trapping PPy membrane in the ESIME module. And then, pouring KI solution (30mL) and pure water (30mL) into source cell chamber and receiver cell chamber, correspondingly. During the continuous extraction process, a pulse potential (+0.95 V/-0.8 V) was performed at the PPy/I_3^- membrane, and a positive cell voltage was performed at the stainless steel plates electrode as displayed in Fig. 1. The samples of the source and receiver cell chambers were collected in the determined periods for the analysis. The ionic fluxes were calculated using the equation (1):

$$\text{Flux} = \frac{(C_1 - C_2)V}{tS} \quad (1)$$

where C_1 and C_2 (mg/L) correspond to the initial and equilibrium concentrations of the ion, respectively, V (L) means the volume of the ion solution, t (h) shows the equilibrium time of the extraction, and S (cm^2) corresponds to the effective membrane area. The selectivity factor (α) for pairs of anions, D and E, was calculated using the following equation:

$$\alpha_{M/N} = \text{Flux of D}/\text{Flux of E} \quad (2)$$

3. Results and discussion

3.1. Morphological and structure characterizations

3.1.1 Morphology observation

Fig. 3 displays the SEM morphologies of SSWM and PPy/I_3^- membrane. One can see that the blank SSWM matrix with a relatively uniform and smooth mesh which size about 38 μm (Fig. 3(a)). From the cross-sectional SEM morphology (Fig. 3(b)), it can be found that the obtained PPy/I_3^- membrane had a thickness of about 100 μm. Moreover, as shown in Figs. 3(c) and 3(d), the PPy/I_3^- membrane was composed of uniform bowl-shape particles (average diameter of about 2 μm) with an interconnected

ant-nest-like structure, which should be benefit for the ion diffusion and transport in the membrane and supply more active sites for the selective extraction of I^- ions. Especially, it is found that the SEM image of this PPy/I_3^- membrane was is markedly different from other ion doped PPy membrane (Fig. S1). The special bowl-shape particles in the PPy/I_3^- membrane could be resulted from the linear structure of I_3^- ions, which could direct the oxidation polymerization process to form the bowl-shape particles. This bowl-shape particle was the bird's nest, which could make a stable space structure system in different levels. In addition, the 3D interconnected porous channels are beneficial to the transport of ions for the ESIME process.

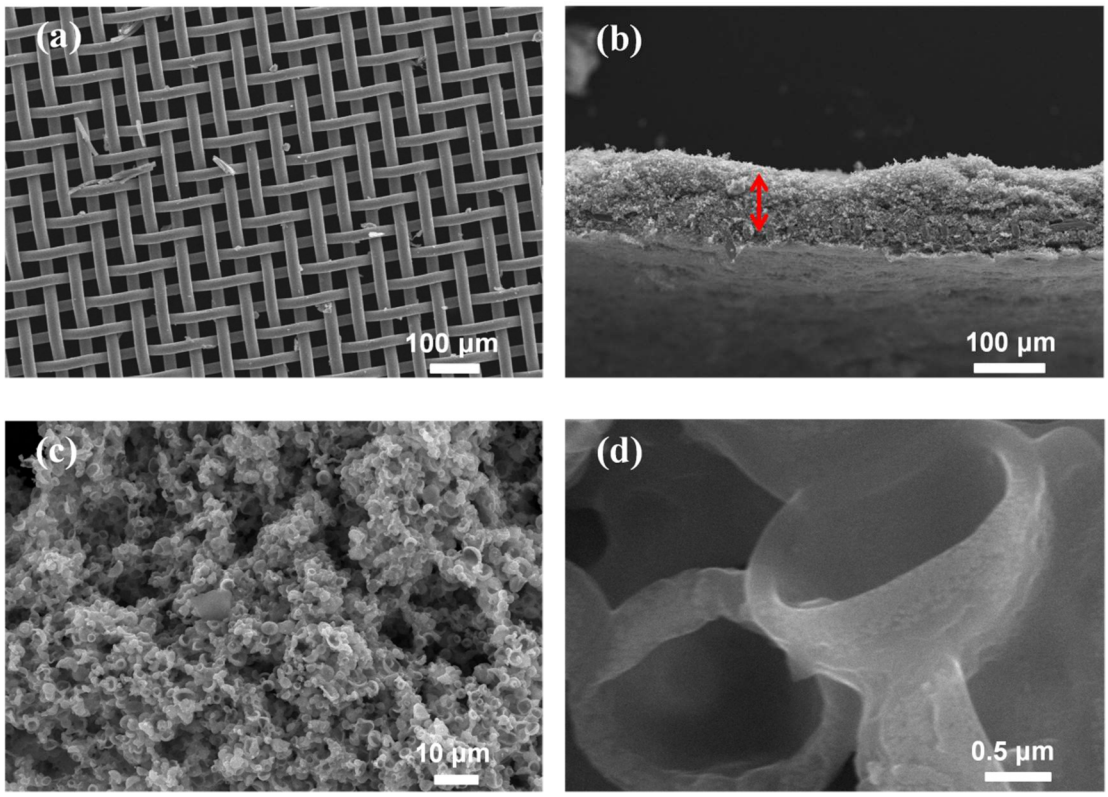

Fig. 3. SEM images of the surface of (a) SSWM matrix, (b) cross section of PPy/I_3^- membrane, (c) (d) PPy/I_3^- membrane at different magnifications.

3.1.2 Structure analysis

Fig. 4(a) shows XRD patterns of *in-situ* PPy/I_3^-, I_3^- ion trapping PPy (after desorption) and I_3^- doped PPy (after extraction). One can see that a broad hump around 23° appeared in the three cases which is attributed to the characteristics diffraction peak of PPy [23, 44], and all of them exhibited similar amorphous 'steamed-bread' peak, which confirmed that the adsorption and desorption of I^- ions did not destroy the membrane structure under the voltage range from 0.95 Vand -0.8 V. Fig. 4(b) shows the corresponding FT-IR spectra of the three states of PPy/I_3^- membrane. Herein, the peak at around 3415 cm^{-1} stands for the typical N-H stretching vibration [45], the peak observed at 1542 cm^{-1} can be signed to C=C stretch of pyrrole ring and the peaks at 1040 cm^{-1} and 904 cm^{-1} are attributed to C-H in-plane and out-plane deformation of the

pyrrole unit, respectively [46, 47]. Meanwhile, the C-N stretching coupled with N-H plane deformation at 1450 cm^{-1}, besides, symmetrical angular deformation of CH_3 at 1290 cm^{-1} [27], and C-N stretching of the amino groups at 1175 cm^{-1} [48] were observed in the three states of PPy/I_3^- membrane, which are corresponding to the characteristic peaks of PPy. In particular, the specific bands of the C-I at 475 cm^{-1} [49, 50] were also observed, and the peak intensity of the C-I bond decreased in the case of the PPy/I_3^- membrane without imprinted I_3^-, which confirmed that I^- ions was successfully removed from the PPy membrane after desorption.

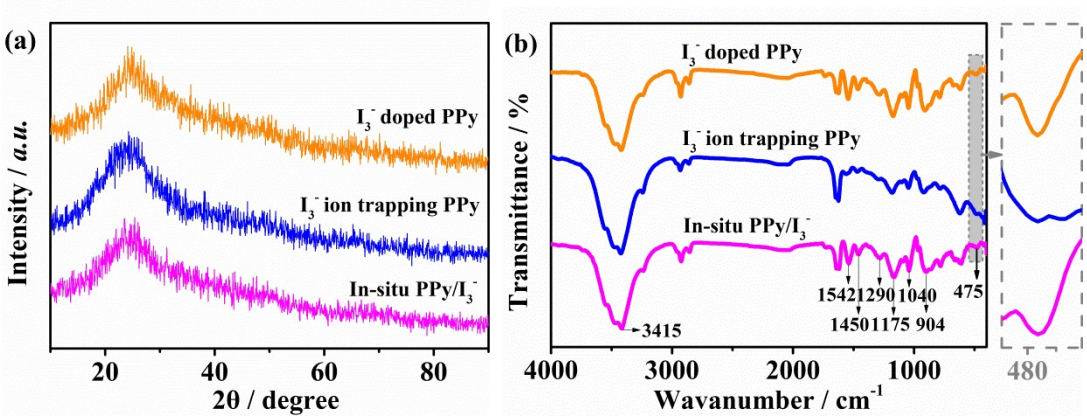

Fig. 4. (a) XRD patterns and (b) FT-IR spectra of PPy/I_3^- membranes under different states.

To further confirm the chemical compositions and element states in the PPy/I_3^- membrane, XPS analysis was performed. The survey XPS spectra (Fig. 5(a)) displayed that three elements of C, N and I were found to be existed in the *in-situ* PPy/I_3^-, I_3^- ion trapping PPy and I_3^- doped PPy. Herein, the peaks of C 1s were identified in the C-C bond at 284.49 eV [2]. As shown in the high-resolution spectrum of I 3d in Fig. 5(b), two pairs of peaks, i.e., 618.3 eV/629.8 eV and 619.9 eV/631.4 eV), were observed for the *in-situ* PPy/I_3^- as well as I_3^- doped PPy, indicating that two iodine species existed in these two case for the PPy/I_3^- membrane, which correspond to the ionic iodine (3d 5/2,

618.3 eV) and covalently bound iodine (3d 5/2, 619.9 eV) [23, 51]. Especially, the covalently bound iodine may be ascribed to I_3^- in the PPy/I_3^- membrane, also suggesting that the oxidation reaction of I^- occurred during the extraction process with I^- ion adsorbed on the PPy/I_3^- membrane. In contrast, after the desorption, only a weaker iodine peak was observed, proving that I_3^- ions were almost completely removed from the membrane, and I_3^- was easily reduced to I^- in the desorption process. The change in the oxidation state of the I^- after the extraction indicated that the PPy/I_3^- membrane had special I_3^- ion trapping ability as indicated above.

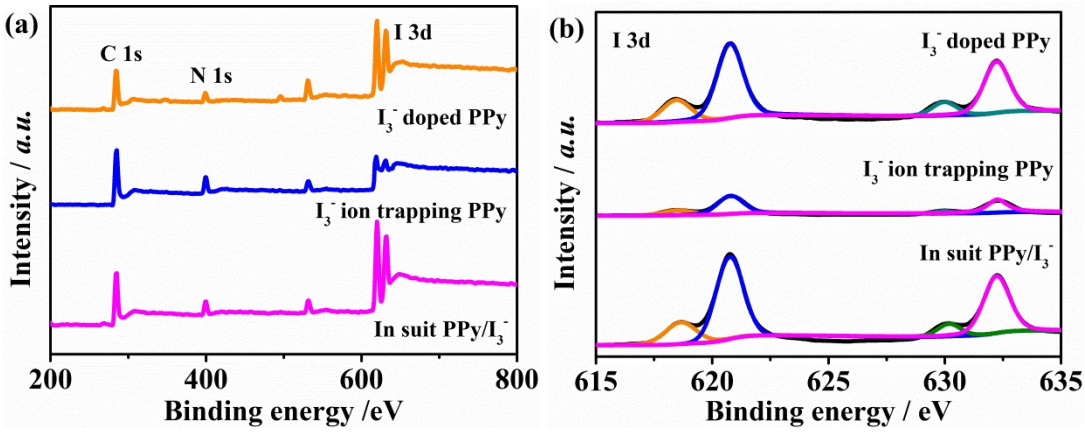

Fig. 5. (a) XPS survey spectrum and (b) XPS spectra of I 3d of PPy/I_3^- membrane under different states.

3.1.3 N_2 adsorption isotherms

Fig. 6(a) shows nitrogen adsorption-desorption isotherms of the I_3^- ion trapping PPy and I_3^- doped PPy. One can see that both of them exhibited a type-II/IV mixed N_2 adsorption/desorption isotherm, demonstrating that the PPy network mainly due to the mesopores and small macropores dominant (Fig. 6(b)), which was also displayd by the pore size distribution analysis by other researchers [52]. The calculated BET surface areas of the I_3^- ion trapping PPy and I_3^- doped PPy were 61.09 $m^2 \cdot g^{-1}$ and 0.88 $m^2 \cdot g^{-1}$, respectively. Obviously, the I_3^- ion trapping PPy had a larger specific surface area,

which can provide rich active sites for the adsorption of I^- ion. On the other hand, after the I^- ions were adsorbed on the membrane, the I_3^- doped PPy displayed a small specific surface area while the total pore volume was also decreased remarkably, proving that I_3^- ions can enter the membrane smoothly so that all the I_3^--binding sites can be fully utilized. These results are also in accordance with the above analyses.

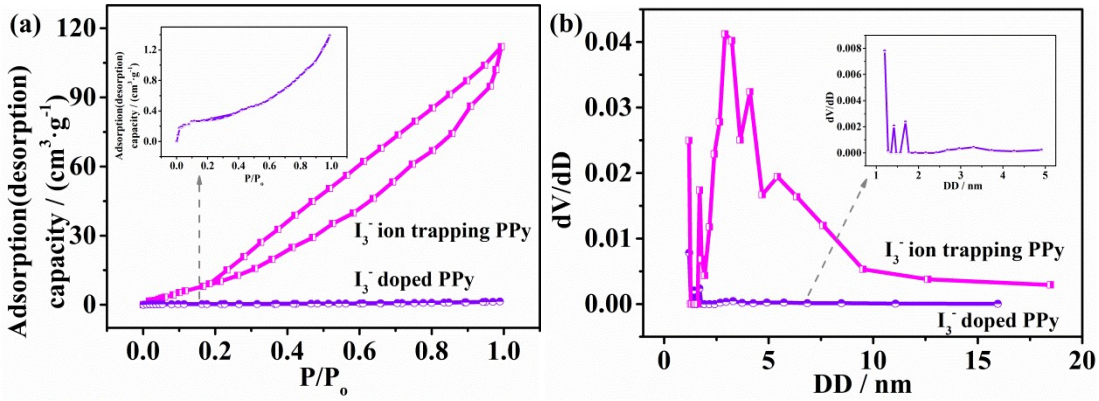

Fig. 6. (a) N_2 adsorption-desorption isotherms and (b) pore size distributions of PPy/I_3^- membrane under different states.

3.1.4 TG analysis

The thermal stability and the degradation behavior of the PPy/I_3^- material was investigated by TG (thermogravimetric) analysis under nitrogen atmosphere. Fig. 7 shows the TG and DTG (differential thermogravimetry) curves of PPy/I_3^- material. The first weight loss was discovered at 40-100 ºC in the TG curve of the PPy/I_3^- material, which assigned to the water elimination. Then, there has an obvious thermal degradation at 150-490 ºC range, which attributed to the sublimation of the trapped I_3^- from the PPy chain structure. Especially, for the I_3^- doped PPy, the hot weightlessness was sharper. Thereafter, an distinct weight loss was discovered at 600-900 ºC range, which attributed to the degradation of PPy. As shown in Fig. 7(b), it should be noted that the degradation behaviors at this range were almost identical in the both cases,

indicating that the adsorption and desorption of I_3^- ions did not affect the PPy structure, which is consistent with the XRD analysis results.

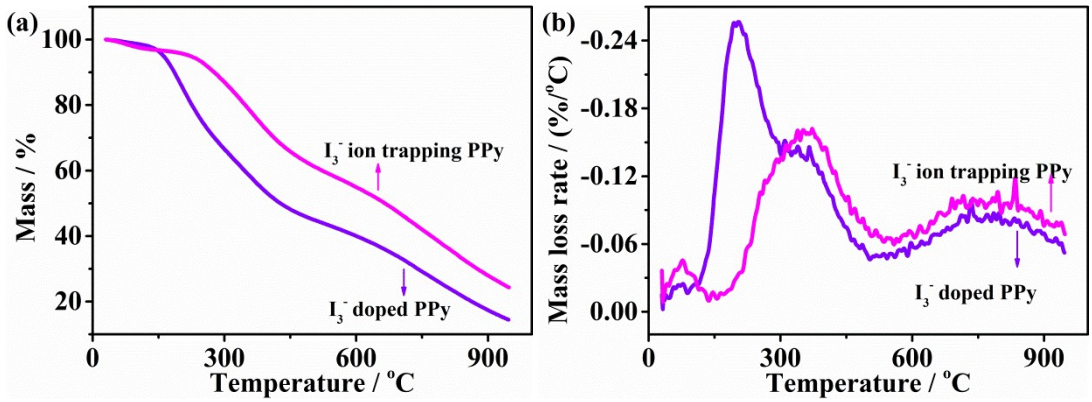

Fig. 7. (a) TG curve and (b) DTG curve of the PPy/I_3^- materials under different states.

3.2 Electrochemical characterization

Fig. 8 manifests the cyclic voltammetry (CV) response of the PPy/I_3^- membrane in 0.1 M KI, KCl, KBr, K_2SO_4 and K_3PO_4 solutions, respectively. Markedly, the CV response of the PPy/I_3^- membrane was more active in the KI solution than the others at the potential range of -0.8 V to -0.95 V, indicating it had higher selectivity toward the target I^- ions due to the ion trapping effect. Moreover, comparing with the imprinting of other anions, more uniform bowl-shape particles with better interconnected ant-nest-like structure were obtained in the PPy/I_3^- membrane (as shown in Fig. S1), which would allow unique ion trapping of I^- ions and faster transfer of the target I^- across the membrane. In addition, the PPy/I_3^- membrane had an obvious oxidation peak in the voltage range from 0.6 to 0.9 V in the KI solution, indicating that I^- ions were firstly oxidized to I_3^- ions and then doped into the membrane, which was confirmed by the above I 3d XPS analysis (Fig. 5(b)), that is, I_3^- doped PPy contained ionic iodine and covalently bound iodine. Furthermore, as shown in Figs. S2 and S3, PPy/I_3^- had a much higher I^- ion adsorption capacity (740 mg·g^{-1}) than the PPy/I^- material (320 mg·g^{-1}).

Thus, it can be concluded that in the extraction process of I^- ions by using the PPy/I_3^- membrane, I^- ions were first oxidized into I_3^- ions, and then captured by the PPy/I_3^- membrane (The specific reaction formula are shown in the supporting material).

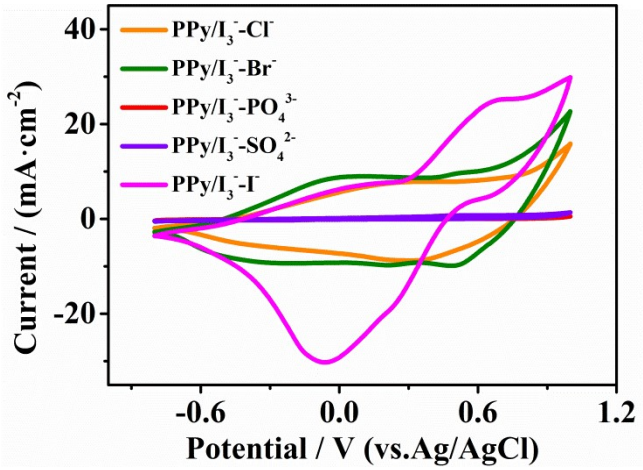

Fig. 8. Cyclic voltammetric responses of PPy/I_3^- membrane in the KI, KCl, KBr, K_2SO_4 and K_3PO_4 solutions respectively with a concentration of 0.1 mol/L for each at a scan rate of 10 mV/s.

3.3 Performance parameters

3.3.1 Effect of cell voltage and pulse width on extraction performance

The effect of cell voltage on the ion extraction process was tested at 0.5 mM KI (source solution) and pure water (receiver solution). As shown in Fig. 9(a), a lower performed cell voltage (0.3 V, 0.6 V, 0.9 V, 1.2 V and 1.5 V) correspond to a smaller flux, and as the applied cell voltage was 1.8 V, a maximum I^- flux was achieved, thereafter, the flux not increase as the cell voltage further increases. Herein, when the applied cell voltage was over 1.8 V, the electrochemical oxidation reaction could occur at the anode electrode, which may affect the extraction of I^- ions, resulting in the decrease of I^- ion flux at a higher cell voltage. On the other hand, when a lower cell voltage was performed, I^- may be desorbed into both the source cell chamber and

receiver cell chamber, thereby, the net I^- flux were comparatively low. Hence, in this study, 1.8 V was chosen as the optimum applied cell voltage.

Pulse width may be a crucial influence factor on the extraction process since it can affect the time of I^- ion adsorption/desorption. Fig. 9(b) shows the effect of the pulse width on the I^- ion flux through the PPy/I_3^- membrane. Obviously, the flux of I^- increased at first and then decreased, herein, a higher I^- ion flux of 2.87×10^{-4} g cm^{-2} h^{-1} was achieved at the 20 s pulse width. Hence, 20 s was considered as the optimal pulse width in this study. Herein, at a shorter pulse time, I^- ions could not enter into the membrane enough to saturate the I_3^--binding sites even at the high potential so that the I_3^--binding sites had trouble filling by I^- ions. That is to say, when immediately changed the high/low potential on the membrane, a lots of ions would be unable to make it and thus be captured by the membrane of PPy, and then desorbed to the receiver cell chamber. As a result, when the pulse width was set at 20 s, the I_3^--binding sites were fully utilized, and the adsorption/desorption of I^- ions can be high-performance completed. However, with a further increase of the pulse time, the I^- ions cannot get into the membrane more, which conversely could affect the expulsion of I^- ions in the whole extraction process. Hence, the optimum pulse width on the ESIME process was selected at 20 s in this study.

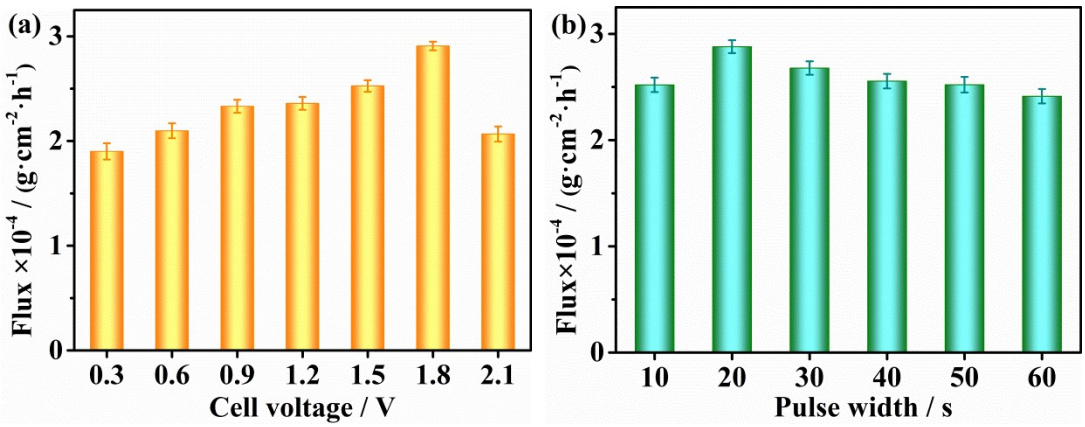

Fig. 9. Effects of cell voltage (a) and pulse width (b) on the flux of I^- ions across the PPy/I_3^- membrane. Pulse potential: -0.8 V/+0.95 V; initial I^- ion concentration: 0.5 $mmol \cdot L^{-1}$.

3.3.2 Effect of initial concentration on extraction process

Fig. 10 shows the effect of I^- ion initial concentration on the extraction flux, in which the pink and blue line were calculated by the decreased concentration of I^- in the source cell chamber and the increased concentration of I^- in the receiver cell chamber, respectively. The results from the data is evident: as the increment of the beginning concentration of I^-, the extraction flux increment, which indicated that the differences of concentration can provide motive for extraction process. Furthermore, it should be noted that the diffusion flux increase with the increase of concentration gradient which conformed to the Fick rule [53]. Moreover, high conductivity of the solution was associated with higher concentration, which could promote the ion migration. Besides, it is found that the increased I^- ions in the receiver cell chamber was a little less than the decreased I^- ions in the source cell chamber for all extraction process, displaying that the I^- ions unable desorbed completely into the receiver cell chamber from the membrane since some of the I^- still caught in the membrane. Furthermore, according to UV analysis, under the performed cell voltage of 1.8 V, only the peak of I^- ions was

detected in the receiver solution, and no peak of I_3^- was found. Therefore, we speculated that in the desorption process, I_3^- should be reduced to I^- before desorption from the membrane (as shown in Fig.1).

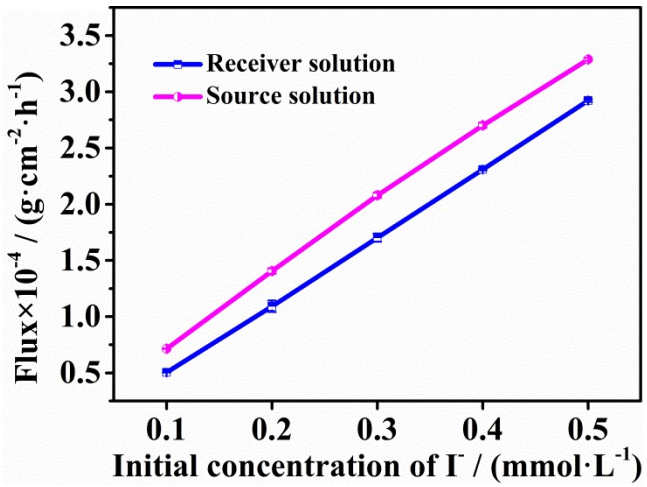

Fig. 10. Effect of the initial concentration on the I^- ion extraction flux across the PPy/I_3^- membrane. Pulse potential: -0.8 V/+0.95 V; cell potential: 1.8 V; pulse width: 20 s.

3.3.3 Effect of ESIME coupling circuit on the I^- extraction process

Fig. 11 shows the concentration vs. time curves during I^- ion extraction in the receiver solution. The four extraction tests (a-d) with different performed conditions demonstrated different results with an I^- ion extraction percentage in the ordered as d>c>b>a. Herein, in case (a), both of cell voltage and pulse potential were not performed. This is natural and expected, both the flux and the extraction percentage of I^- ions were very low since the extraction of I^- was only used differences in the concentration of ions within the two solutions to do work. Besides, the interaction between the PPy and I^- (rather than I^{3-}) was fairly puny. Thus, a low extraction percentage (≤12.4%) was obtained in this case. In case (b), a cell voltage was performed to the stainless steel sheets electrodes but without a pulse potential, so that an uniform

external electric field was formed in the entire cell chamber. As such, the anions should be attracted to the anode in the receiver cell chamber whereas the cations to the cathode in the source cell chamber. As a result, due to the electric field provided additional driving force for I^- ion extraction, the I^- ions flux was higher than that in case (a). Nonetheless, the extraction rate of I^- ($\leq$32.4%) was still lower than the expected. In case (c), only a pulse potential was performed on the PPy/I_3^- membrane but no cell voltage on the electrode. One can see that the flux of I^- was improved to some extent when compared with the cases (a) and (b) since the adsorption/desorption of I^- can be enhanced by the pulse potential applied on the PPy/I_3^- membrane. But the extraction percentage of I^- ions was also as low as 33.4% since the absence of the external electric field to drive I^- ions transferred across the membrane. Thus, I^- ions could be released to both sides of the source and receiver cell chamber. In case (d), a novel ESIME process with a pulse potential on the PPy/I_3^- membrane and a cell voltage was performed on the electrodes. The results showed that the flux and the extraction rate of I^- ions were both markedly improved to as high as 83.3%, achieving continuous and efficient I^- extraction, which was dramatically higher than the sum of rates from (b) and (c). In this case, more importantly, I^- ions should be firstly oxidized into I_3^- ions, which can be rapidly captured by the positively charged PPy/I_3^- membrane and then desorbed from the negatively charged PPy/I_3^- membrane in the form of I^- ions since the perform of the pulse potential on the PPy/I_3^- membrane. In other words, the capture and desorption of I^- ions should be accurately controlled by the high/low pulse potential of the PPy/I_3^- membrane, which will affect the efficiency of ion extraction. Meanwhile, the electric field applied on the cell can strongly drive the captured I^- ions through the membrane, enhancing their migration from the source cell chamber to the membrane and then to the receiver cell chamber. Therefore, the synergistic effect of ESIME process resulted

in the continuous extraction of I^- with high efficiency and enhanced extraction percentage in the case (d).

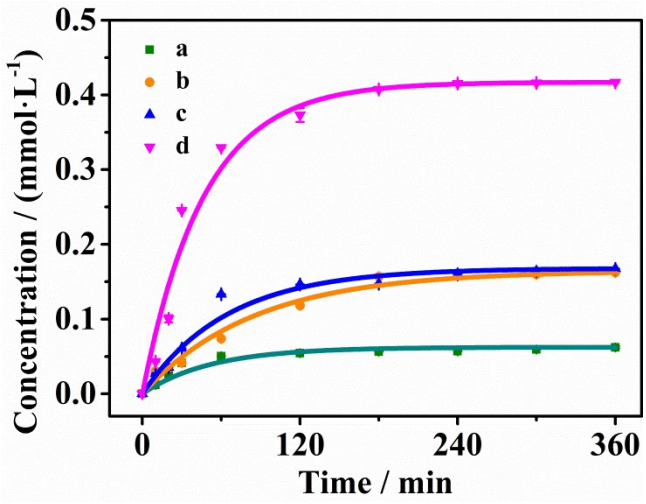

Fig.11. Concentration vs. time curves during I^- ion extraction in the receiver solution (H_2O, pH =7). (a) No any potentials were applied on the cell and the PPy/I_3^- membrane; (b) only 1.8 V cell voltage was performed; (c) only a pulse potential of -0.8 V/+0.95 V was performed on the PPy/I_3^- membrane, and (d) 1.8 V voltage on the cell and pulse potential of -0.8 V/+0.95 V on the PPy/I_3^- membrane were applied. Pulse width: 20 s; initial I^- concentration: 0.5 mmol·L^{-1}.

3.4 Selectivity of PPy/I_3^- membrane

The selectivity of the PPy/I_3^- membrane for I^- extraction was tested with the ESIME system at a 30 mL mixed solution containing I^-, Cl^-, Br^-, SO_4^{2-} and PO_4^{3-} (0.5 mmol/L each) under a cell voltage of 1.8 V, a pulse potential of -0.8 V/0.95 V with a pulse width of 20 s and an extraction time of 3 h. As displayed in Fig. 12, the anion fluxes cross the PPy/I_3^- membrane were in the order as $I^- > Br^- > Cl^- > SO_4^{2-} > PO_4^{3-}$, and the extraction capacity of I^- ions was much higher than any other anion. The separation factors of I^- over Br^-, Cl^-, SO_4^{2-} and PO_4^{3-} were calculated as 3.44, 3.98, 5.02 and 5.27 (Table 1). As discussed above, the PPy/I_3^- membrane demonstrated specific

I_3^--binding sites with the C-I bond (as shown in Fig. 4(b)), which should be benefit for the selective capture of I^- ions. In addition, the eminent selectivity towards I^- ions was also consistent with CV results (Fig. 8), in which the PPy/I_3^- membrane exhibited more excellent electrical activity in I^- ions solution.

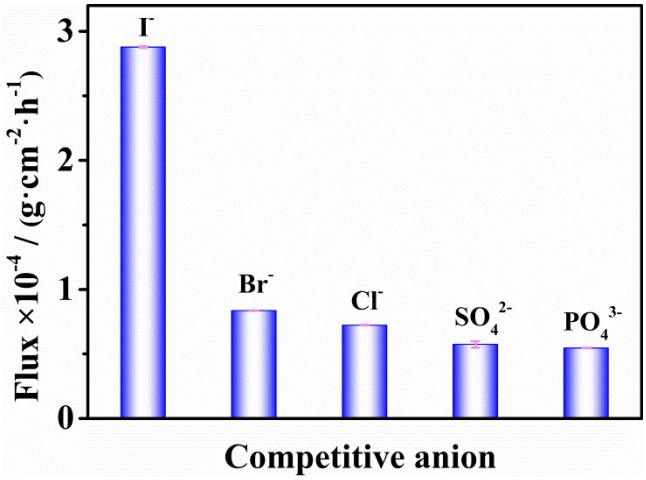

Fig. 12. Flux of I^- through PPy/I_3^- membrane in the ESIME system with a 30 mL mixed solution including I^-, Cl^-, Br^-, SO_4^{2-}, and PO_4^- ions. (The amount of each anion: 0.5 mmol·L^{-1}. Pulse potential: -0.8 V/+0.95 V; cell potential: 1.8 V; pulse width: 20 s for 180 min).

Table 1. Fluxes and separation factors of the PPy/I_3^- membrane for I^- ions with other competitive anions.

Ions type	I^-	Br^-	Cl^-	SO_4^{2-}	PO_4^{3-}
Flux×10^{-4} (g cm^{-2} h^{-1})	2.87	0.83	0.72	0.59	0.54
Separation factor	1	3.44	3.98	5.02	5.27

3.5 Stability of PPy/I_3^- membrane

The performance stability of PPy/I_3^- membrane was tested in the ESIME system under the optimum conditions. Herein, the PPy/I_3^- membrane was reused for 10 times. After each extraction test, the membrane and cell chamber were washed with pure water at first, and then the fresh solutions were poured into cell chambers. The extraction rates for the PPy/I_3^- membrane in the stability test are displayed in Fig. 13. Notably, no apparent decrease of extraction percentage had been observed as the device working continuously for 10 times. Rather, in the first and second cycles, the extraction rates were slightly lower than the following cycles. It is possible that some I^- ions might be trapped in the inner membrane in the initial 2 cycles, which cannot completely desorbed in to the receiver solutions. Importantly, an extraction efficiency of 94.8% was still reached after recycle used for several times, which demonstrated that the PPy/I_3^- membrane had excellent stability performance. As stated above, the obtained PPy/I_3^- membrane had unique 3D interconnected special structure, which can ensure the fast diffusion of the I^- ions across the membrane and provide the space for the swelling and shrinking changes during the pulse potential applying process. Hence, the unique 3D interconnected ant-nest-like structure in PPy/I_3^- membrane applied in the ESIME system demonstrated an preeminent stability performance.

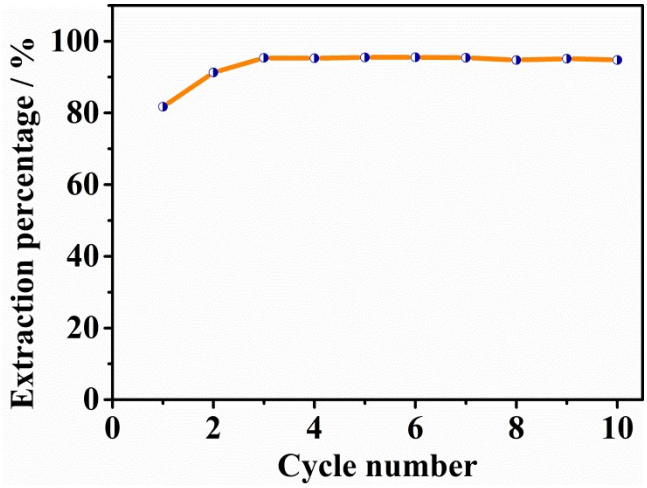

Fig. 13. Extraction percentages for the PPy/I_3^- membrane during the recycle using test for I^- ions. (Pulse potential: -0.8V/+0.95 V; cell potential: 1.8 V; pulse width: 20 s; initial I^- ion concentration: 0.5 mmol·L^{-1} for 180 min).

4. Conclusions

A novel ESIME system with an electroactive PPy/I_3^- membrane composed of uniform bowl-shape particles with an interconnected ant-nest-like structure was successfully developed for the extraction of I^- ions from the aqueous solutions. It is considered that the I^- redox reaction occurred in the special triiodide ion trapping PPy/I_3^- membrane during the I^- ion extraction process, which played a key role in the selective extraction of I^- ions. Meanwhile, the ESIME process with a pulse potential on the PPy/I_3^- membrane and a cell voltage applied to the system significantly enhanced the flux of I^- and realized high-efficiency continuous extraction of I^- ions. The PPy/I_3^- membrane exhibited a superior flux of 2.87×10^{-4} g·cm^{-2}·h^{-1} at the performed conditions with a cell voltage of 1.8 V, a pulse potential of -0.8 V/+0.95 V, a pulse width of 20 s. Moreover, the extraction percentage reached as high as 94.8% after several recycle using processes. It is expected that such an ESIME process with the PPy/I_3^- membrane

may be an outstanding candidate for the high-efficiency continuous extraction of target I^- ions from industrial water systems.

Acknowledgements

This work is supported by the National Natural Science Foundation of China (21776191 and 21706181), the National Key R&D Program of China (No. 2017YFE0129200 and 201803D421094) and JSPS KAKENHI Grant 19K12395, Japan, Scientific and Technologial Innovation Programs of Higher Education Institutions in Shanxi (No. RD1900000627).

References

[1] Y. Xiong, B. Dang, C. Wang, H. Wang, S. Zhang, Q. Sun, X. Xu, Cellulose fibers constructed convenient recyclable 3D graphene-formicary-like delta-Bi_2O_3 Aerogels for the selective capture of iodide, ACS Appl. Mater. Inter. 9 (2017) 20554-20560.

[2] S. Han, W. Um, W.S. Kim, Development of bismuth-functionalized graphene oxide to remove radioactive iodine, Dalton. T. 48 (2019) 478-485.

[3] L.Q. Peng, W.Y. Yu, J.J. Xu, J. Cao, Pyridinium ionic liquid-based liquid-solid extraction of inorganic and organic iodine from laminaria, Food Chem. 239 (2018) 1075-1084.

[4] R.X. Yao, X. Cui, X.X. Jia, F.Q. Zhang, X.M. Zhang, A luminescent zinc(II) metal-organic framework (MOF) with conjugated pi-electron ligand for high iodine capture and nitro-explosive detection, Inorg. Chem. 55 (2016) 9270-9275.

[5] Y. Zhu, Y.J. Ji, D.G. Wang, Y. Zhang, H. Tang, X.R. Jia, M. Song, G. Yu, G.C. Kuang, Bodipy-based conjugated porous polymers for highly efficient volatile iodine capture, J. Mater. Chem. A 5 (2017) 6622-6629.

[6] S. Xiong, X. Tang, C. Pan, L. Li, J. Tang, G. Yu, Carbazole-bearing porous organic polymers with a mulberry-like morphology for efficient iodine capture, ACS Appl. Mater. Inter. 11 (2019) 27335-27342.

[7] P. Wang, Q. Xu, Z. Li, W. Jiang, Q. Jiang, D. Jiang, Exceptional iodine capture in 2D covalent organic frameworks, Adv. Mater. (2018) e1801991.

[8] K. Jie, Y. Zhou, E. Li, Z. Li, R. Zhao, F. Huang, Reversible iodine capture by nonporous pillar[6]arene crystals, J. Am. Chem. Soc. 139 (2017) 15320-15323.

[9] K.W. Chapman, P.J. Chupas, T.M. Nenoff, Radioactive iodine capture in silver-containing mordenites through nanoscale silver iodide formation. J. Am. Chem. Soc. 132 (2010), 8897-8899.

[10] R. Fernández de Luis, A. Martínez-Amesti, E.S. Larrea, L. Lezama, A.T. Aguayo, M.I. Arriortua, Composite β-$AgVO_3$@$V1.6^{5+}V0.4^{4+}O4.8$ hydrogels and xerogels for iodide capture, J. Mater. Chem. A 3 (2015) 19996-20012.

[11] B. Valizadeh, T.N. Nguyen, B. Smit, K.C. Stylianou, Porous metal-organic framework@polymer beads for iodine capture and recovery using a gas-sparged column, Adv. Funct. Mater. 28 (2018) 1801596.

[12] Z. Tauanov, V.J. Inglezakis, Removal of iodide from water using silver nanoparticles-impregnated synthetic zeolites, Sci. Total. Environ. 682 (2019) 259-270.

[13] W. Zhang, Q. Li, Q. Mao, G. He, Cross-linked chitosan microspheres: an efficient and eco-friendly adsorbent for iodide removal from waste water, Carbohyd. Polym. 209 (2019) 215-222.

[14] S. Choung, M. Kim, J.S. Yang, M.G. Kim, W. Um, Effects of radiation and temperature on iodide sorption by surfactant-modified bentonite, Environ. Sci. Technol. 48 (2014) 9684-9691.

[15] C. Li, Y. Wei, X. Wang, X. Yin, Efficient and rapid adsorption of iodide ion from aqueous solution by porous silica spheres loaded with calcined Mg-Al layered double hydroxide, J. Taiwan Inst. Chem. E. 85 (2018) 193-200.

[16] A. Bo, S. Sarina, Z. Zheng, D. Yang, H. Liu, H. Zhu, Removal of radioactive iodine from water using Ag_2O grafted titanate nanolamina as efficient adsorbent, J. Hazard. Mater. 246-247 (2013) 199-205.

[17] S. Liu, N. Wang, Y. Zhang, Y. Li, Z. Han, P. Na, Efficient removal of radioactive iodide ions from water by three-dimensional Ag_2O-Ag/TiO_2 composites under visible light irradiation, J. Hazard. Mater. 284 (2015) 171-181.

[18] X. Zhang, P. Gu, S. Zhou, X. Li, G. Zhang, L. Dong, Enhanced removal of iodide ions by nano Cu_2O/Cu modified activated carbon from simulated wastewater with improved countercurrent two-stage adsorption, Sci. Total. Environ. 626 (2018) 612-620.

[19] P. Mao, Y. Liu, Y. Jiao, S. Chen, Y. Yang, Enhanced uptake of iodide on Ag@Cu_2O nanoparticles, Chemosphere 164 (2016) 396-403.

[20] P. Mao, L. Qi, X. Liu, Y. Liu, Y. Jiao, S. Chen, Y. Yang, Synthesis of Cu/Cu_2O hydrides for enhanced removal of iodide from water, J. Hazard. Mater. 328 (2017) 21-28.

[21] M. Sancho, J.M. Arnal, G. Verdú, J. Lora, J.I. Villaescusa, Ultrafiltration and reverse osmosis performance in the treatment of radioimmunoassay liquid wastes, Desalination 201 (2006) 207-215.

[22] F.L. Theiss, G.A. Ayoko, R.L. Frost, Iodide removal using LDH technology, Chem. Eng. J. 296 (2016) 300-309.

[23] S. Liao, C. Xue, Y. Wang, J. Zheng, X. Hao, G. Guan, A. Abuliti, H. Zhang, G. Ma, Simultaneous separation of iodide and cesium ions from dilute wastewater based

on PPy/PTCF and NiHCF/PTCF electrodes using electrochemically switched ion exchange method, Sep. Purif. Technol. 139 (2015) 63-69.

[24] D.K.L. Harijan, V. Chandra, T. Yoon, K.S. Kim, Radioactive iodine capture and storage from water using magnetite nanoparticles encapsulated in polypyrrole, J. Hazard. Mater. 344 (2018) 576-584.

[25] J. Li, M. Wang, G. Liu, L. Zhang, Y. He, X. Xing, Z. Qian, J. Zheng, C. Xu, Enhanced iodide removal from water by nano-silver modified anion exchanger, Ind. Eng. Chem. Res. 57 (2018) 17401-17408.

[26] Z. Ye, L. Chen, C. Liu, S. Ning, X. Wang, Y. Wei, The rapid removal of iodide from aqueous solutions using a silica-based ion-exchange resin, React. Funct. Polym. 135 (2019) 52-57.

[27] Z. Guo, M. Shams, C. Zhu, Q. Shi, Y. Tian, M.H. Engelhard, D. Du, I. Chowdhury, Y. Lin, Electrically switched ion exchange based on carbon-polypyrrole composite smart materials for the removal of ReO_4^- from aqueous solutions, Environ. Sci. Technol. 53 (2019) 2612-2617.

[28] J. Xing, C. Zhu, I. Chowdhury, Y. Tian, D. Du, Y. Lin, Electrically switched ion exchange based on polypyrrole and carbon nanotube nanocomposite for the removal of chromium(VI) from aqueous solution, Ind. Eng. Chem. Res. 57 (2018) 768-774.

[29] S. Zhang, Y. Shao, J. Liu, I.A. Aksay, Y. Lin, Graphene-polypyrrole nanocomposite as a highly efficient and low cost electrically switched ion exchanger for removing ClO_4^- from wastewater, ACS Appl. Mater. Inter. 3 (2011) 3633-3637.

[30] X. Du, G. Guan, X. Li, A.D. Jagadale, X. Ma, Z. Wang, X. Hao, A. Abudula, A novel electroactive λ-MnO_2/PPy/PSS core-shell nanorod coated electrode for selective recovery of lithium ions at low concentration, J. Mater. Chem. A 4 (2016) 13989-13996.

[31] X. Du, H. Zhang, X. Hao, G. Guan, A. Abudula, Facile preparation of ion-imprinted composite film for selective electrochemical removal of nickel(II) ions, ACS Appl. Mater. Inter. 6 (2014) 9543-9549.

[32] Y. Yang, X. Du, A. Abudula, Z. Zhang, X. Ma, K. Tang, X. Hao, G. Guan, Highly efficient defluoridation using a porous MWCNT@NiMn-LDH composites based on ion transport of EDL coupled with ligand exchange mechanism, Sep. Purif. Technol. 223 (2019) 154-161.

[33] J. Wang, F. Gao, X. Du, X. Ma, X. Hao, W. Ma, K. Wang, G. Guan, A. Abudula, A high-performance electroactive PPy/rGO/NiCo-LDH hybrid film for removal of dilute dodecyl sulfonate ions, Electrochim. Acta (2019) 135288.

[34] J. Luo, X. Du, F. Gao, Y. Yang, X. Hao, S. Li, X. Hao, K. Tang, G. Guan, Iodide ion trapping polypyrrole film: selective capture of iodide ions by electrochemically switched ion extraction (ESIE) process, Chem. Eng. J. 380 (2020) 122529.

[35] X. Du, D. Zhang, X. Ma, W. Qiao, Z. Wang, X. Hao, G. Guan, Electrochemical redox induced rapid uptake/release of Pb(II) ions with high selectivity using a novel porous electroactive HZSM-5@PANI/PSS composite film, Electrochim. Acta 282 (2018) 384-394.

[36] F. Gao, X. Du, X. Hao, S. Li, X. An, M. Liu, N. Han, T. Wang, G. Guan, An electrochemically-switched BPEI-CQD/PPy/PSS membrane for selective separation of dilute copper ions from wastewater, Chem. Eng. J. 328 (2017) 293-303.

[37] F. Gao, X. Du, X. Hao, S. Li, J. Zheng, Y. Yang, N. Han, G. Guan, A potential-controlled ion pump based on a three-dimensional PPy@GO membrane for separating dilute lead ions from wastewater, Electrochim. Acta 236 (2017) 434-442.

[38] F. Gao, X. Du, X. Hao, S. Li, J. Zheng, Y. Yang, N. Han, G. Guan, Electrical double layer ion transport with cell voltage-pulse potential coupling circuit for separating dilute lead ions from wastewater, J. Membrane Sci. 535 (2017) 20-27.

[39] F. Gao, X. Du, X. Hao, X. Ma, L. Chang, N. Han, G. Guan, K. Tang, A novel electrical double-layer ion transport carbon-based membrane with 3D porous structure: high permselectivity for dilute zinc ion separation, Chem. Eng. J. 380 (2020) 122413.

[40] P. Zhang, J. Zheng, Z. Wang, X. Du, F. Gao, X. Hao, G. Guan, C. Li, S. Liu, An in situ potential-enhanced ion transport system based on FeHCF-PPy/PSS membrane for the removal of Ca^{2+} and Mg^{2+} from dilute aqueous solution, Ind. Eng. Chem. Res. 55 (2016) 6194-6203.

[41] M. Menkuer, H. Ozkazanc, Electrodeposition of polypyrrole on copper surfaces in OXA-DBSA mix electrolyte and their corrosion behaviour, Prog. Org. Coat. 130 (2019) 149-157.

[42] X. Du, X. Hao, Z. Wang, G. Guan, Electroactive ion exchange materials: current status in synthesis, applications and future prospects. J. Mater. Chem. A 4 (2016), 6236-6258.

[43] C. Weidlich, K.M. Mangold, K. Jüttner, Continuous ion exchange process based on polypyrrole as an electrochemically switchable ion exchanger, Electrochim. Acta 50 (2005) 5247-5254.

[44] H. Mi, X. Zhang, X. Ye, S. Yang, Preparation and enhanced capacitance of core-shell polypyrrole/polyaniline composite electrode for supercapacitors, J. Power Sources 176 (2008) 403-409.

[45] D. Jose, R. Joseph, H. John, Synthesis, characterization, morphological and electrical studies of polypyrrole nanostructures, AIP Conference Proceedings 2082 (2019) 030011.

[46] S. Yalçınkaya, C. Demetgül, M. Timur, N. Çolak, Electrochemical synthesis and characterization of polypyrrole/chitosan composite on platinum electrode: Its electrochemical and thermal behaviors, Carbohyd. Polym. 79 (2010) 908-913.

[47] M.J. González-Tejera, M.L. De Plaza, E.D. Sánchez La Blanca, I. Hernández-fuentes, electrochemical, FTIR and morphological study of polypyrrole-polystyrenesulphonate conducting films. Polym. Int. 31 (1993), 45-50.

[48] P. Wang, X. Du, T. Chen, X. Hao, A. Abudula, K. Tang, G. Guan, A novel electroactive PPy/HKUST-1 composite film-coated electrode for the selective recovery of lithium ions with low concentrations in aqueous solutions, Electrochim. Acta 306 (2019) 35-44.

[49] D. Mansuroglu, I.U. Uzun-Kaymak, Enhancement of electrical conductivity of plasma polymerized fluorene-type thin film under iodine and chlorine dopants, Thin. Solid Films 636 (2017) 773-778.

[50] J. Morales, M.G. Olayo, G.J. Cruz, R. Olayo, Plasma polymerization of random polyaniline-polypyrrole-iodine copolymers, J. Appl. Polym. Sci., 85 (2002) 263-270.

[51] C. Wochnowski, S. Metev, UV-laser-assisted synthesis of iodine-doped electrical conductive polythiophene. Appl. Surf. Sci. 186 (2002), 34-39.

[52] P. Mu, H. Sun, T. Chen, W. Zhang, Z. Zhu, W. Liang, A. Li, A sponge-like 3D-PPy monolithic material for reversible adsorption of radioactive iodine, Macromol. Mater. Eng. 302 (2017) 1700156.

[53] K. Malek, M.O. Coppens, Knudsen self-and fickian diffusion in rough nanoporous media, J. Chem. Phys. 119 (2003) 2801-2811.